# Numerical Analysis and Reinforcement Management of Slopes

Zhiqiang Chen [1, a]

[1] Northwest Research Institute Co.,Ltd of C.R.E.C, China

[a] 2320610908@qq.com

**Abstract.** In order to manage a roadside landslide, a qualitative and quantitative stability analysis of the main landslide face was carried out based on the ground investigation data; a numerical analysis model was constructed to analyze the stress field, displacement field and stability coefficient change of the main landslide face, which verified the reliability of the results from qualitative and quantitative analyses; a numerical calculation was carried out to analyze the stress field calculation and stability coefficient change of the formulated "Anchor + Drainage" reinforcement scheme; the feasibility and reliability of the reinforcement scheme were also verified. Numerical calculations were used to calculate the stress field, displacement field and stability coefficient changes of the proposed "anchor + cut-off drainage" reinforcement scheme, which verified the feasibility and reliability of the reinforcement scheme. The results show that: (1) the qualitative and quantitative analysis results are relatively reliable, and the stability coefficient of the slope before reinforcement does not meet the requirements of the engineering specification, which indicates that the slope is unstable and there is a risk of deformation damage. (2) The average stress and displacement changes of the slope after reinforcement are significantly reduced, and the average stress and displacement of the anchors are increased, indicating that the reinforcement program effectively prevents the deformation and sliding of the slope. (3) The stability coefficient of the slope after reinforcement is improved by 25.9% relative to that before reinforcement, indicating that the reinforcement scheme is feasible.

**Keywords:** numerical; finite element; stability; reinforcement; treatment.

## 1. Introduction

As a hot issue in the field of geotechnical engineering, slope stabilization and management has been widely concerned by many experts and scholars [1-5]. PENG Wenzhe et al [6] explored the general rule of slope stability change under pile foundation loading and proposed the corresponding stability coefficient calculation method; WU Dongting [7] used finite element software to comparatively analyze the stability of a slope reinforced by skidding piles under different working conditions; TIAN Kun et al [8] investigated the role of lateral shear effect of soil nail-supported clayey slopes on the stability of the slopes in engineering practice; ZHENG Qiyin et al [9] comparatively investigated the slope stability changes under different anti-slip pile anchorage positions and depth conditions; ZHANG Bangxin et al [10] comparatively investigated the reinforcement effect of different reinforcement schemes based on the sensitivity analysis of geotechnical body parameters.

Numerical simulation, as an important technical means for slope stability analysis, plays an important role in assisting the verification of calculation results and adjusting the management program. By constructing a finite element model and simulating the field working conditions in the form of constrained loading, real-time tracking analysis of slope stability changes can be realized. In this paper, we constructed a slope finite element model based on the field investigation data, compared and analyzed the stress field, displacement field and stability coefficient changes before and after the slope reinforcement, and verified the feasibility of the proposed reinforcement scheme, and the analysis results have certain reference value for similar projects.

## 2. Project overview

The slope project is located in Chaozhou City, Guangdong Province, for a high-speed branch section of the road side slope. The slope area belongs to the old landslide range, affected by continuous rainfall, the geotechnical properties deteriorate, and the downward force of the slope body increases. The landscape of the slope area is low hills, the elevation is between 180m~480m, the relative height difference is about 300m, among which the elevation of the back edge of the landslide is about 350m, the elevation of the front edge is about 190m, the relative height difference is about 160 m. The slope gradient is mostly 15~30°, average is about 17°. The full view of the slope is shown in Fig. 1.

Fig. 1 General view of the slope

## 3. Stability analysis

### 3.1 Qualitative evaluation

During the geological mapping process, no obvious signs of deformation of the old landslide were found. Comprehensive drilling and monitoring results found that the back edge of the landslide has obvious misplaced platform formation, clear perimeter, and loose slope surface. Although it has been counter-pressured, it is still creeping and deforming according to the surface monitoring data, and it is judged that the engineering landslide is in the creeping stage (unstable state).

### 3.2 Quantitative evaluation

3.2.1 Parameter selection

The weight of the landslide body is mainly determined according to the experience parameters and geotechnical tests in the area; the strength indexes c and Φ of the soil body on the sliding surface (belt) are mainly determined by referring to the experience parameters, geotechnical tests and inverse algorithms in the area in the past. Referring to the previous investigation data and combining with the results of this investigation and test, the average natural capacity of the landslide body of the selected engineering landslide and the old landslide is 18KN/m³, and the average saturated capacity is 19.5KN/m³, and the average natural capacity of the landslide body of the selected potential deep-seated landslide is 18.5KN/m³, and the average saturated capacity is 19.5KN/m³. On the basis of the deformation activity characteristics and corresponding stability degree of each possible landslide surface before the implementation of this landslide management project, combined with relevant experimental and empirical parameters, the mechanical indexes of the main landslide surface were back-calculated, and the calculation results are shown in Table 1.

Table 1. Backcalculation parameters

| placement | Calculation section | state of affairs | subsoil | | | landslide | note |
|---|---|---|---|---|---|---|---|
| | | | place | cohesive force | friction angle | Average natural capacity | |

| | | | | C/kPa | φ/（°） | γ /(KN/m$^3$) | |
|---|---|---|---|---|---|---|---|
| DZK19+740 ～ DZK19+940 | main slide | natural state | main slide of a landslide | 20 | 24 | 19 | Comprehensive parameters |
| | | | trailing edge traction section | 0 | 35 | 19 | empirical parameter |

3.2.2 Selection of calculation section

Combined with the site investigation information, the main slip surface of the slope was selected as shown in Fig. 2.

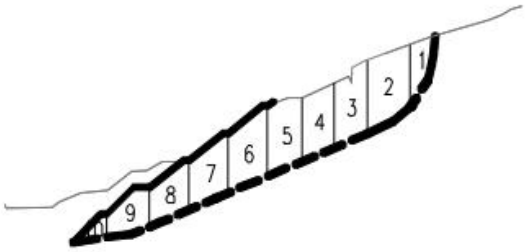


Fig. 2 Calculated section of the main slip surface

3.2.3 Stability calculation

According to the material and structural characteristics of the slide, the signs of deformation and the morphology of the folded slip surface, the transfer coefficient method is used to calculate the stability of the computational model according to the theory of rigid-body limit equilibrium. Combined with the ground investigation data around the slope, it is determined that the seismic intensity of the slope area is VII degree zone, i.e., the influence of horizontal seismic force is introduced to analyze the stability of the main slip face of the slope under natural working condition, and the calculation formula is shown in equation (1).

$$Fs=\frac{\sum(c_i\Delta L_i cos\alpha_i+W_i tg\varphi_i)\left[cos\alpha_i+\left(\mathrm{tg}\varphi_i sin\alpha_i/F_s\right)\right]^{-1}}{\sum W_i sin\alpha_i} \quad (1)$$

Where: $F_s$——slope stability coefficient;

$W_i$——the weight of the ith block side slope soil bar, unit: kN;

$\alpha_i$——angle of inclination of soil strip of the $i$-th block of slope, unit: °;

$c_i$——cohesive force of the $i$-th block, unit: kPa;

$\varphi_i$——friction angle of block $i$, unit: °.

The stability coefficient of the main slip surface of the slope is calculated to be 1.02, referring to the relevant engineering specifications, it is determined that the section is in an unstable state.

## 4. Numerical analysis

### 4.1 Model construction

Through site investigation and field drilling, the geological structure of the main section of the slope was determined as shown in Fig 3, and the physical and mechanical parameters of the geotechnical body were determined by indoor and outdoor tests as shown in Table 2.

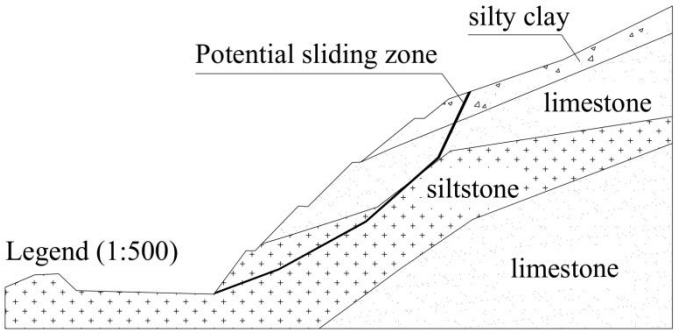


Fig. 3 Geologic structure of the main section

Table 2. Physical and mechanical parameters

| Category | Severe/(kN.m$^{-3}$) | Cohesion/kPa | Friction angle/(°) | Modulus of elasticity/MPa | Poisson's ratio |
|---|---|---|---|---|---|
| sliding belt | 18 | 16.5 | 12 | 14 | 0.3 |
| powdery clay | 20 | 23 | 16.4 | 15 | 0.35 |
| siltstone | 22 | 21 | 25 | 300 | 0.37 |
| limestone | 21.5 | 27 | 26.5 | 320 | 0.32 |
| Anchor | - | - | - | 200000 | 0.35 |

Combining the geological structure of the main section and the physical and mechanical parameters of its different geotechnical bodies, the numerical analysis model of the main section of the slope is constructed based on the Moore-Cullen theory and finite element theory as shown in Fig. 4. Horizontal and vertical displacement constraints are imposed on the bottom surface of the model, horizontal displacement constraints are imposed on both sides, and the rest are free boundaries. The slope is meshed using plane strain (CPE4) cell type.

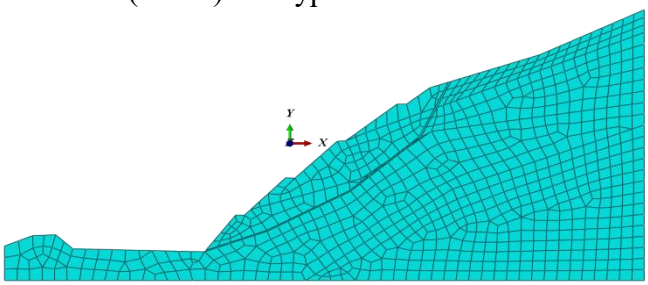

Fig. 4 Finite element model

### 4.2 Numerical calculations

The intersection point of grade 4 slope and platform of the section is selected as the tracking research point, and the inflection point of the displacement of the tracking point is taken as the judgment criterion of slope instability, based on the constructed finite element model, the stress field, displacement field and stability change of the main section of the slope are analyzed. The calculated stress and displacement cloud diagrams and slope stability coefficient change curves are shown in Fig. 5, Fig. 6 and Fig. 7, respectively.

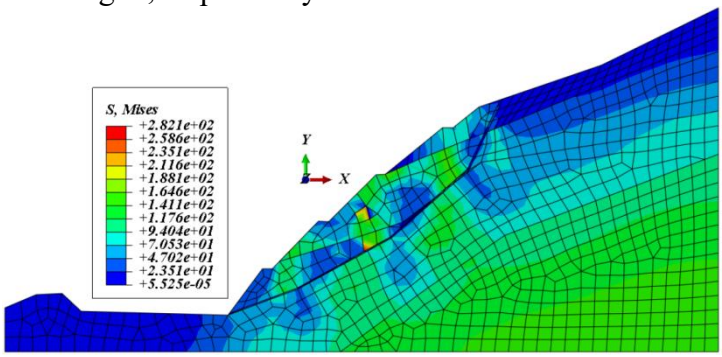


Fig. 5 Stress cloud diagram

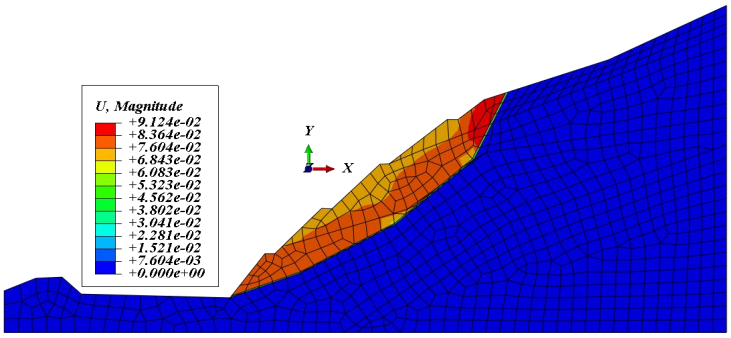


Fig. 6 Displacement cloud map

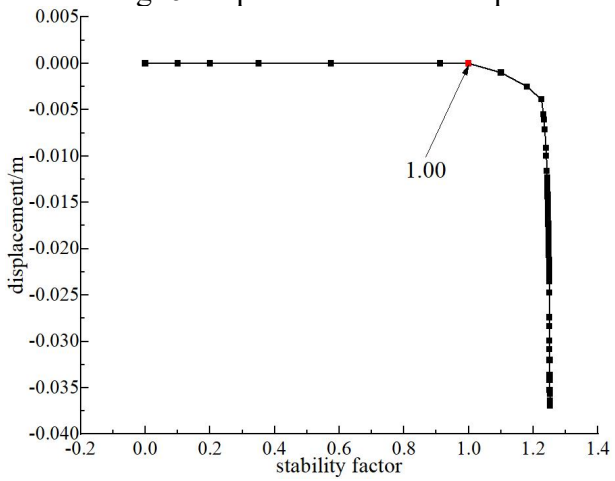


Fig. 7 Stability coefficient variation curve

From Fig. 5 to 7, it can be seen that: the average stress in the region of powdery clay at the top of the slope and sandstone at the foot of the slope is smaller than that in the region of the sliding zone and its upper part and the region of muddy powdery sandstone in the interior of the slope body; the maximum value of the average stress is 282.1Pa, which is located in the region of the upper part of the sliding zone, and the minimum value of the average stress is $5.525\times10^{-5}$Pa, which is located in the region of the top of the slope and the foot of the slope. The slope sliding area is located in the sliding zone and the area above it with the maximum displacement value of 9.124 cm, while the rest of the area is relatively stable with minimal displacement. The tracking study point on the slope surface has a sudden change when the stability coefficient is 1.00, i.e., the stability coefficient of the main section is 1.00, while the engineering standard stipulates that such slopes satisfy the stability requirements when the stability coefficient reaches 1.2~1.3 in the natural working condition, which indicates that the main section of the slope is unstable and needs to be reinforced and treated.

## 5. Reinforcement

Through expert analysis and discussion, it was determined to adopt the reinforcement and management plan of "anchor + intercepting and draining", in which anchors of different lengths were laid from the foot of the slope along the slope to the top of the slope, respectively.4 rows of anchors are laid on the slope of level 1, the length of which is 11.5m, and the angle with the horizontal plane is 25°; 3 rows of anchors are laid on the slope of level 2, the lengths of which are 17m, 17m and 17.5m from the bottom upwards; 3 rows of anchors are laid on the slope of level 3, the lengths of which are 20m, 20.5m and 21m from the bottom upwards; 3 rows of anchors are laid on the slope of level 4, the lengths of which are 13m, 13.5m and 14m from the bottom upwards; a cut-off gutter is poured with C20 concrete at the top of the slope. 14m, at the top of the slope using C20 concrete pouring interceptor ditch, the specific layout as shown in Fig. 8.

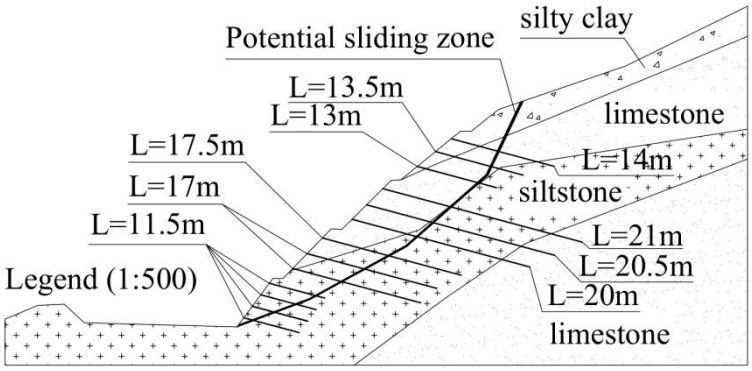


Fig. 8 Reinforcement Program

The finite element model is constructed as shown in Fig. 9, with horizontal and vertical displacement constraints applied at the bottom and horizontal displacement constraints applied at both sides; the anchor and slope body are built-in constraints; the slope body is meshed with the plane strain (CPE4) cell type, and the anchor is meshed with the truss (T2D2) cell type; and the main cross section of the reinforced slope is analyzed in terms of the stress field and the displacement field. The stress and displacement maps and stability coefficient change curves of the slope and anchors are shown in Fig. 10 to Fig. 12, respectively. The tracking research point which is consistent with the one before reinforcement is selected, and the sudden change of the displacement of the tracking point is used as the criterion to judge the stability of the slope body, and the stability coefficient change curve of the reinforced slope body is shown in Fig. 13.

From Fig. 10 to Fig. 13, it can be seen that: the average stress change of the slope body after reinforcement is small, the average stress change is mainly concentrated in the area of the anchor, the maximum average stress reaches $1.146\times10^{6}$kPa, and the average stress change of the anchor is the minimum of 37.87Pa, which indicates that the anchor plays an important role in the prevention of slope sliding; the slope sliding range is still concentrated in the sliding zone and the area above it, and the maximum displacement of the anchor is 5.059mm, which is 94.5% lower than that before reinforcement. The maximum displacement of the anchor is 5.014mm, indicating that the overall displacement of the slope is significantly reduced after reinforcement, and the anchor effectively prevents the deformation of the slope damage; after reinforcement, the displacement of the tracking point in the stability coefficient reaches 1.35 when the mutation, that is, the stability coefficient of the slope body is 1.35 to meet the requirements of the engineering specification, and relative to the pre-stabilization increased by 25.9%, indicating that the reinforcement program is feasible.

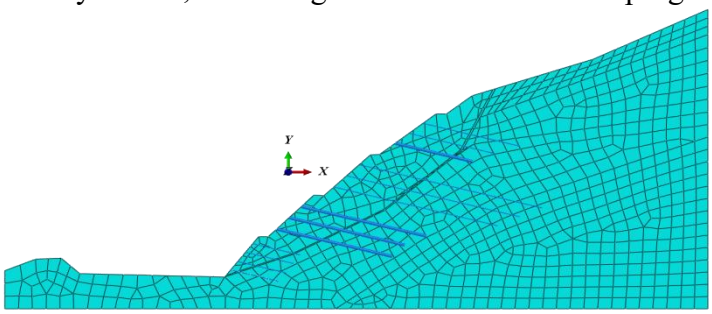


Fig. 9 Finite element model of the reinforcement scheme

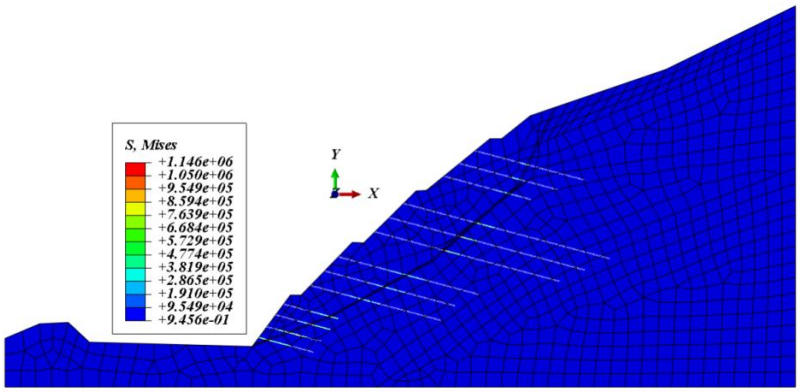


Fig. 10 Stress cloud after reinforcement

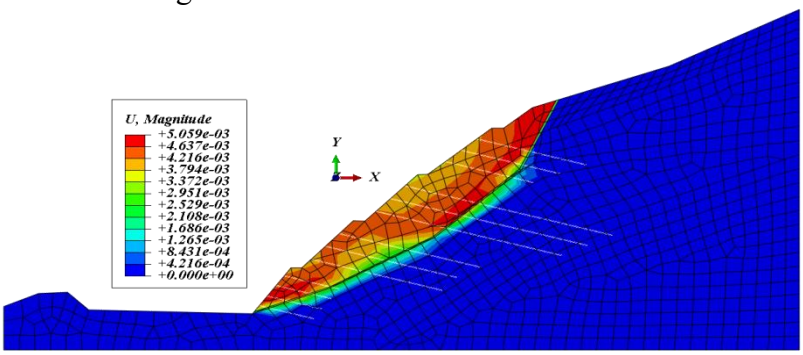


Fig. 11 Displacement cloud after reinforcement

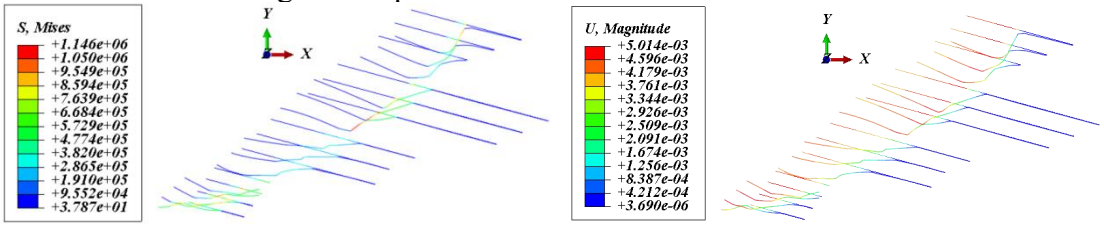


Fig. 12 Variation of anchor stress and displacement

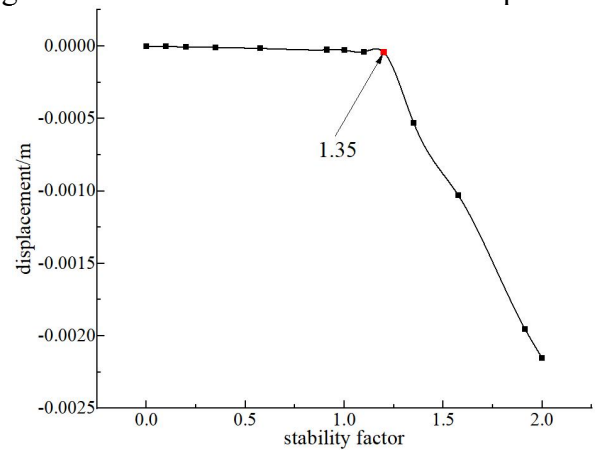


Fig. 13 Variation curve of slope stability coefficient after reinforcement

## 6. Conclusion

(1) The stability coefficient of the main section of the slope before reinforcement is 1.02 by qualitative and quantitative analysis, and the result of numerical analysis is 1.02, which indicates that the results of qualitative and quantitative analysis are relatively reliable; the results of the analysis don't meet the requirements of the engineering specification, i.e., the slope is unstable, and there is a risk of deformation and damage.

(2) The average stress change of the slope after reinforcement is significantly reduced, and the average stress change is mainly distributed on the anchor rods, and the maximum value of slope displacement is reduced by 94.5%, which indicates that the anchor rods effectively prevent the slope from deformation and sliding.

(3) The stability coefficient of the main section of the slope after reinforcement is 1.35, which is 25.9% higher than that before reinforcement, and 24.4% higher than that of the quantitative analysis results, indicating that the reinforcement program is feasible.

## Acknowledgments

This work was financially supported by National Key R&D Project (2022YFC3002603), Chongqing Natural Science Foundation Upper-level Project (CSTB2023NSCQ-MSX0878), Major Science and Technology Special Project/Key R&D Task Special Project of the Autonomous Region (2022B03033-2)

## References

[1] JIANG Wei, QI Zhiyu, DENG Huafeng, et al. Damage mechanism and stability of soft and hard interbedded anticlinal rocky slopes in reservoir area under the condition of deterioration of rock mass at the foot of slope. Journal of Civil Engineering, 2023, 56(S1): 181-193.

[2] LUO Junyao, ZHU Guojin, FENG Yelin, et al. Engineering geological characteristics and stability evaluation of flood discharge exit slopes of GS hydropower station. Materials Herald, 2023, 37(S2): 283-289.

[3] ZHAO Lianheng, ZHAO Weilong, WEI Bin, et al. Upper limit analysis of homogeneous slope stability based on three-parameter damage criterion. Journal of Hunan University (Natural Science Edition), 2023, 50(7): 188-199.

[4] YANG Xuehui, LU Fa, GUO Nan, et al. Stability calculation and numerical simulation analysis of multistage loess high slope. Journal of Geotechnical Engineering, 2022, 44(S1): 172-177.

[5] WANG Shichuan, SAN Gangqing. Numerical analysis of stability of folded slopes reinforced by anti-slip piles. Highway, 2022, 67(12): 73-81.

[6] PENG Wenzhe, ZHAO Minghua, YANG Chaowei. Slope stability under pile foundation loading based on finite element limit analysis. Journal of Hunan University (Natural Science Edition), 2022, 49(11): 189-197.

[7] WU Dongting. Analysis of seismic stability of slopes reinforced by anti-slip piles. China Highway, 2022, 8(22): 100-103.

[8] TIAN Kun, ZHU Hongguang, ZHANG Chengcheng. Influence of lateral shear effect of soil nails on slope stability. Journal of Engineering Geology, 2022, 30(5): 1744-1752.

[9] ZHENG Qiyin. Analysis of anchorage position and depth of skid pile based on Midas/GTS. China Highway, 2022, 12(20): 118-120.

[10] ZHANG Bangxin, JIA Jianqing, LIU Zhongshuai, et al. Stability analysis of Xiafen slope and its management measures. Journal of Lanzhou Jiaotong University, 2023, 42(1): 9-15.